Res Chem Intermed (2015) 41:2393–2405
DOI 10.1007/s11164-013-1354-2

Chemical interaction, interfacial effect and the microstructural characterization of the induced zinc–aluminum–*Solanum tuberosum* in chloride solution on mild steel

O. S. I. Fayomi · A. P. I. Popoola

Received: 20 March 2013 / Accepted: 27 July 2013 / Published online: 14 August 2013

Abstract In this study, we report the effect of *Solanum tuberosum* (ST) as a strong additive on the morphological interaction, wear, and hardness properties of electroplated zinc coating in chloride bath solutions. The structural and the mechanical behavior of the Zn–Al–ST coating were studied and compared with the properties of Zn coatings. Characterization of the electrodeposited coatings were carried out using scanning electron microscopy, energy dispersive spectrometer, AFM, and X-ray diffraction techniques. The adhesion between the coatings and substrate was examined mechanically using hardness and wear techniques. From the results, amorphous Zn–Al–ST coatings were effectively obtained by electrodeposition using direct current. The coating morphology was revealed to be reliant on the bath composition containing strong leveling additives. From all indications, ST content contribute to a strong interfacial surface effect leading to crack-free and better morphology, good hardness properties, and improved wear resistance due to the precipitation of Zn_2Si and $Zn_7Al_2Si_3$. Hence, addition of ST is beneficial for the structural strengthening, hardness, and wear resistance properties of such coatings.

Keywords Chemical interaction · *Solanum tuberosum* · Microstructural · Co-deposition · AFM · Interface

Introduction

The application of steel for the advancement of engineering components in industries cannot be over-emphasized due to its exceptional properties. Because of its importance as an engineering material, there have been unending efforts by

O. S. I. Fayomi (✉) · A. P. I. Popoola
Department of Chemical, Metallurgical and Material Engineering, Surface Engineering Research Centre, Tshwane University of Technology, P.M.B. X680, Pretoria, South Africa
e-mail: ojosundayfayomi3@gmail.com

researchers to prevent its degradation caused by its susceptibility to corrosion attacks [1–5]. Among the preventive measures have been electrodeposition techniques especially using zinc-based coatings and other zinc alloy matrix coatings such as Zn–Ni, Zn–Co, Zn–Fe, Zn–Al, Zn–Cd, Zn–TiO_2, and Zn–Ni–TiO_2.

The use of additives in electrodeposition has also been one of the major factors in predicting the performance of coatings, because they tend to change the morphology, reduce porosity, and assist in better corrosion resistance properties [5–13]. Most inorganic and metallic composite additives, such as thiourea, glycerin, SiC, PTFE, MoS_2 Mg, and Sn to mention but a few, have been reported to provide such characteristics. However, their toxicity, availability, and cost of purchase have limited local producers of coated components and this has led to this investigation into the use of green and organic juice extracts as alternative additives [14–17].

Recently, there has been great interest in the study of the electrodeposition of Zn and other co-deposited matrices in the presence of natural and organic additives in order to improve morphological appearance and to enhance adhesive and leveling effects of coated materials [18]. The beneficial effect of the natural additives as reported in the literature is enormous. Their contributions are considered to provide unique structures on coatings, fine grain particles, and the absence of porosity within the interface [16, 17, 19–23].

One severe challenge of the coating structure is the existence of inner micro-cracks and signs of stress, which have been reported to be reduced by the addition of natural juice extracts, inhibitors/additives, and pure dispersed particulates in the plating bath condition [22, 24–26]. Detailed studies on the effect of organic additives, such as sugarcane and cassava juice extracts, on the mechanical and corrosion behavior of Zn electrodeposition on mild steel shows that inclusion of natural juice extracts reduced stress formation and impact stability on the surface morphology [16].

Here, we attempt to study the interaction and impact of *Solanum tuberosum* (ST) extracted juice on the plating bath formation and coating properties. ST is used in corrosion inhibition techniques to provide corrosion resistance and reduce degradation. It serves as a wetting surfactant which is capable of reducing surface tension. Also, organic compounds have been discovered as brightening agents in electroplating. In addition, they contain complex ion and minerals, as well as glucose and sucrose. They have phytonutrient vitamins and thus pose no detrimental effect on the environment or as a hazard to human health.

In this study, the surface morphology, tribological behavior, and hardness properties of a Zn–Al–ST coating were investigated and compared to those of ordinary Zn coatings having taken into consideration the chemical constituents of ST complex ions.

Experimental

Material preparation

The electroplating setup containing the Zn–Al–ST formulation was attained through a plating bath containing two working anodes and a cathode (substrate). Mild steel

samples of 40 mm × 20 mm × 1 mm with the chemical composition shown in Table 1 were used as substrate and 99 % zinc sheets of 30 mm × 20 mm × 1 mm were used as anodes. AR grade chemicals were used throughout. Deionized water was used for the admixed preparation of the bath solution. The surface preparation of the mild steel sample was done with different grades of emery paper in the order of 60, 120, 400, 800 and 1,600 μm to erase any existing marks. The polished specimens were further pickled in dilute HCl acid solution to remove all organic contaminants and oxides. Electrolytic degreasing was carried out by treating the surface of the samples with an alkaline solution by passing a current for 5 min and consequently cleaning in water.

Methods

The prepared metal substrate was immersed in a solution containing dissolved bath constituents of admixed salts. The cathodes and the anode were connected to the negative and positive terminals of the rectifier, respectively, with a voltage of 1.0 V and 0.2 A for 20 min with the depth of immersion and distance from cathode to anode kept constant. Immediately after the plating, rinsing was done in distilled water and samples were air-dried. The chemical composition of the mild steel is shown in Table 1. The natural potato tuber (*Solanum tuberosum*) used was obtained from a shop in Pretoria, South Africa, with the molecular structure shown in Fig. 1. The preparation process parameters are shown in Table 2.

Extracted fermentation process

Potato tubers weighing 2 kg were collected. The tubers were cut into smaller pieces and blended using a blending machine. The blended tubers were then soaked in 500-ml containers containing ethanol. The solution was then filtered and left to evaporate at room temperature for 4 days to produce a highly concentrated juice extract. The ST tuber extract was stored in clean airtight bottles and refrigerated.

Characterization of the electrodeposited samples

Surface characterization

The surface morphology of the electrodeposits was observed using a scanning electron microscope (SEM/EDS) (model: Joel 6100). The EDX attached to the SEM was used to analyze the coating composition. X-ray diffraction (XRD) analysis was also conducted to examine the coating phase change and crystals. The surface

Table 1 Chemical composition (wt%) of mild steel substrate

Element	C	Mn	Si	P	S	Al	Ni	Fe
% Composition	0.15	0.45	0.18	0.01	0.031	0.005	0.008	Balance

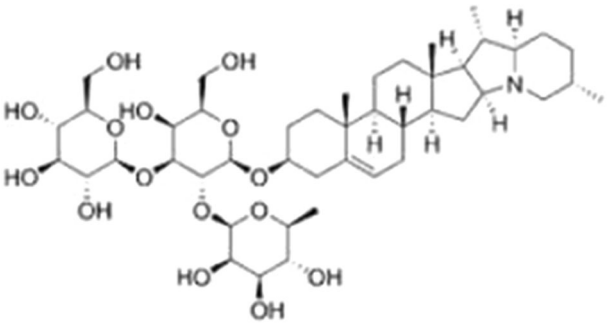

Fig. 1 Molecular structure of *Solanum tuberosum*

Table 2 Composition of the Zn–10 % ST plating bath

Composition	Concentration (g/l)
$ZnSO_4$	120
KCl	80
Al fine particle	10
H_3BO_4	20
ST	10 %
T (°C)	25
pH	4.5

topography and adhesion properties were explained with the help of an atomic force microscope (AFM). Micro-hardness studies were carried out using a Diamond pyramid indenter EMCO Test Dura-scan 10 micro-hardness tester at a load of 10 g for a period of 20 s. Measurements were taken along the cross-section region of the plated film sample toward the substrate.

Abrasive wear test

Three body abrasive wear tests were performed on an ASTM-G65-04 dry sand rubber wheel apparatus. Figure 2 shows a schematic of the wear test set-up. Silica sand procured from Rolfes Silica with a particle size between 300 and 600 μm was used as the abrasive material and set to a flow rate of 7.89 g/s. An applied load of 20 N and a rotational wheel speed of 120 revs/min was used. All samples were abraded for 30 min to evaluate the mass loss.

Results and discussion

Influence of extracted juice product

The undeveloped bath solution provided a coarse dull deposit between the current density of 2 A/dm^2 at 1 V. To develop the nature of the deposit, ST was added to

the chloride bath solution. The nature of the coating was improved at a concentration of 10 ml of ST. From all indications, a bright deposit at 20 min gave better crystals. Critical observation on the concentration of ST in the bath solution shows that the deposit was bright over a current density range of 2 A. Meanwhile, this is assumed and expected since surfactants are used in electrodeposition to control the metallic crystal shape and size in order to produce smooth and bright deposits [27, 28]. The general physiochemical features of the deposit are mostly understood, including their adsorption phenomena and surfactant molecular activities.

Influence of potassium chloride

Potassium chloride was added to increase the conductance of the bath solution. The concentration of potassium chloride was kept constant at 80 g/l in the bath solution. The deposit was bright over the current density of 2 A/dm^2.

Influence of boric acid

Homogeneous compounds and absorbed effects of boric acid was observed in this work as reported by Elsherief and Shoeib [10]. It was observed that boric acid either complexes with Al^{3+} and Zn^{2+}, acting as a regular reactor, or adsorbs on the bath resulting in significant surface morphology and better compositional features. In addition, the presence of boric acid increase the tendency of the deposition process efficiency with the help of other depositional parameters.

Influence of Al dispatch in deposit

The common positive effects of additives are mostly to change and cause the preferred deposit orientation, which can support the chemical, physical, and

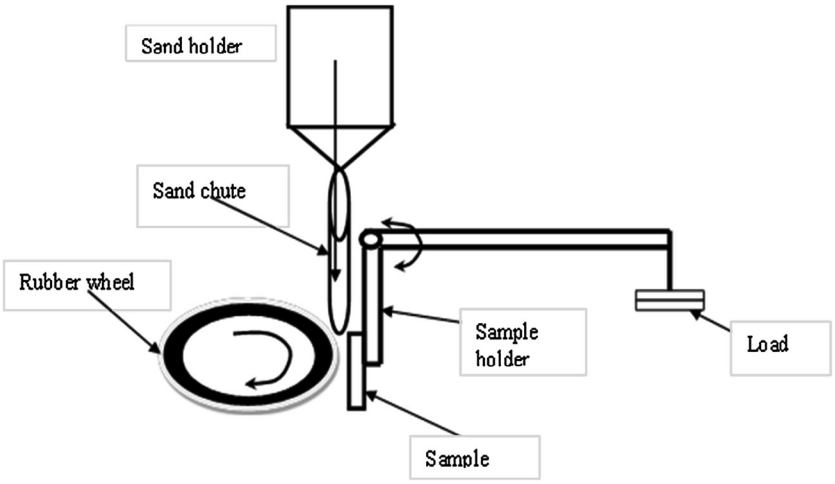

Fig. 2 Schematic diagram of abrasive wear tester

mechanical characteristics of the coating [17, 29–31]. Subsequently, this is in line with this study where the minor percentage of aluminium in the admixed chloride bath changes the crystal structure tremendously giving rise to the increase in corrosion polarization and better adhering nuclei precipitation of the coating. In other words, the solubility of Al and its occurrence as the oxide $Al(OH)_3$ in the solution may provoke a tendency of corrosion products to be formed at the metal/solution interfaces of the alloy. Hence, it is affirmed by Popoola et al. [5] and Basavanna et al. [32] that formation of this existing particulate or composite may, in fact, be the main reason for the occurrence of diffusion behavior in the interface of any alloy or coated sample.

SEM/EDS surface characterization of deposited sample

Figure 3a, b shows the scanning electron micrographs and attached EDs of the substrate and Zn coating. The nature of the surface crystal and orientation in Fig. 3b revealed the non-homogeneous appearance, and some obvious cracks and porosities round the surface morphologies. It was also observed that co-deposition was not uniform, as stress appeared in the coating due to the absence of a stress-relief agent. The little adhesion that occurs within the interface is as a result of the presence of boric acid and the conductance, although deposition was made but adhesion was not as satisfactory as expected. Popoola et al. [5] and Amuda et al. [6] suggested that the phenomenon of adhesion, bright surface, and small porosity of the coating for zinc deposition could also be possibly attributed to the coating parameters such as time of immersion, the potential involved, and the concentration of the normal additive and conductance, which may not have been sufficient in the bath to produce better deposition. However, in the case of Zn with Al–ST in Fig. 4, the situation was different.

The presence of metallic dispatched precipitation of Al was visible. More important is the significant improvement on the surface modification of the coating, as it has also been reported by Elsherief and Shoeib [10] that the growth of a coating is controlled by the nucleation. In another vein, the Al particulate adheres on the cathode surface subsequently acting as a vital nucleation agent to cover the nucleation sites and further alter the movement of the Zn–Al matrix growth. It is noteworthy that the existence of additive particulates improves the modification of crystal size and regulates the uniform morphology of the crystals. It is always well said about electrocodeposition phenomena that thin coatings exhibit lower surface roughness which is in line with the findings in this study in which the additive in the form of surfactant, absorbent and intermetallic particles not only improves surface morphology but also facilitates strong adhesion of the thin films over the substrate.

On the other hand, the concentration of the additive and correct plating time could be vital to the thermodynamic stability of bath formation to facilitate fine grain particles, good leveling behavior and porosity-free sites. The chemical composition of the ST juice was complex with effective chemical compounds and minerals such as sucrose which have been reported to be effective addition levelers

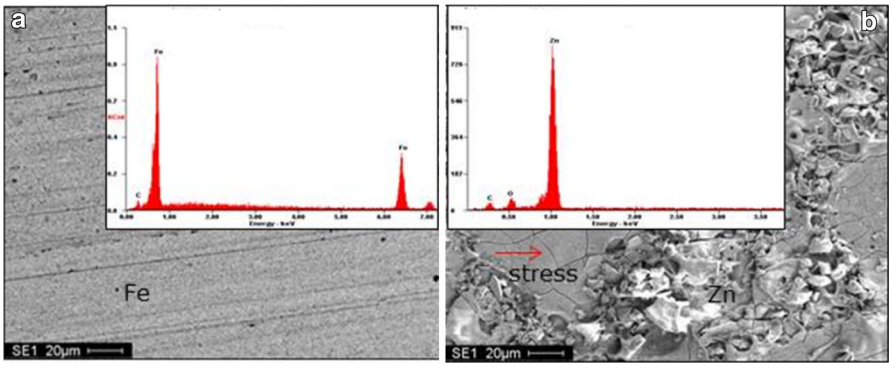

Fig. 3 SEM/EDS micrographs of **a** mild steel, **b** Zn without additive

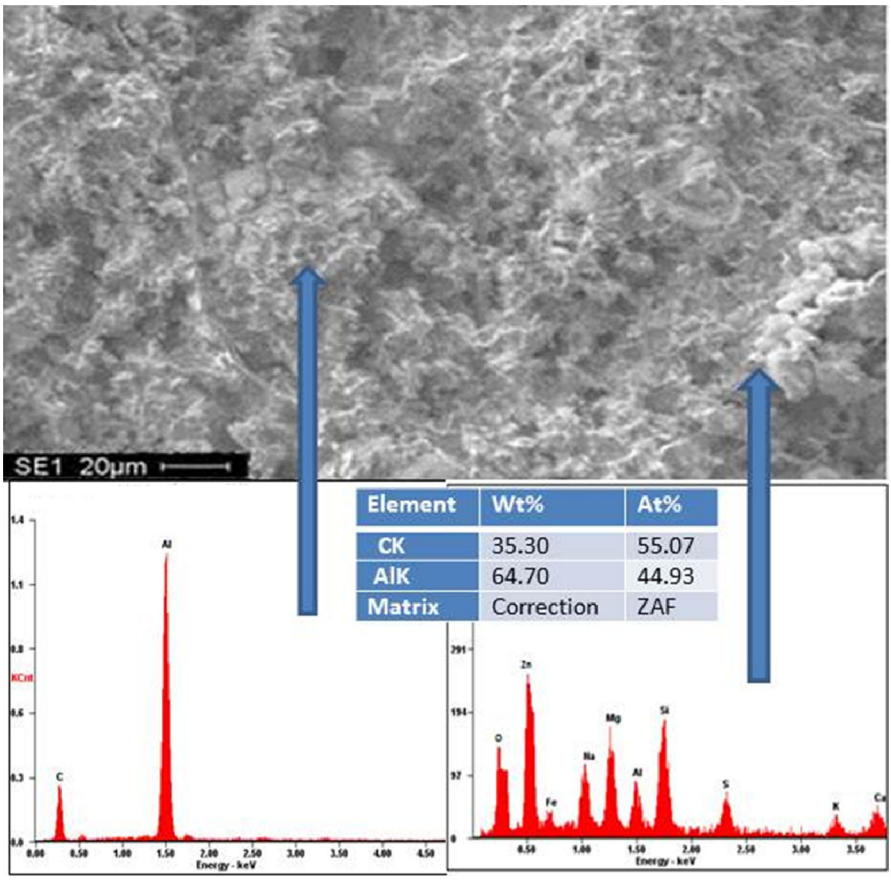

Fig. 4 SEM/EDS of Zn–Al–ST

and agents for zinc plating [21]. This robust phyto-complex compound and particulates could also make a support to the change in surface modification through nuclei replenishment, intermetallic reaffirming, and blocking tendency of the loss sites. Likewise, the adsorption molecules of ST and metallic Al particles in the presence of other bath conductance could also be a major kinetics force to provide a strong bond to the compatibility and surface strengthening of the coating.

Similarly, EDX examination achieved on the deposit indicate that Zn, Al and other chemical complex constituents reflect the existence of the inclusion of an additive agent. Therefore, reinforcing particles represented with juice extract in this work are anticipated.

XRD analysis

In order to appraise the impact of the aluminium and extract on the efficiency and content on the morphology, X-ray diffraction analysis was used as shown in Fig. 5, and it revealed that the zinc-based coatings were solid solutions of zinc–aluminium. Additionally, an influence of the aluminum and juice complexes content on the crystal orientation was found. Zn, Zn–AlO, Zn_2Al_{13}·Sn, and ZnAl crystal phases were recognized in the coating interface. The unique precipitation of Zn_2Al_{13}·Sn phase content was assumed to be the reason for the better adhesion.

Wear behavior of the developed coating

The wear study of Zn in the presence of deposited fine Al metals and ST was carried out. Figure 6 shows the graphs of the variation of the wear rate as a function of time for all the samples, as-received and Zn and Zn–Al–ST depositions, respectively. The rate of wear is very high for the as-received sample; on the other hand, we have very low wear rate loss from the electrolytic Zn–Al–ST followed by that of zinc. This great influence may be attributed to the high notch of particles traveled from the bath through the influence of the applied voltage as a result of the good throwing power and the conditioning of the bath formulation. It can also be said that the existence of aluminum inclusion and extract enhanced the wear resistance and most importantly reduced wear loss as observed in our previous study [4, 5].

In addition, SEM/EDS micrographs of the worm surfaces of the coating sre illustrated in Figs. 7 and 8. A reduced degree of plastic deformation, grooves and little pull-out was noted on the Zn–Al–ST which is assumed to be as a result of the organic extract which lowered the surface interfacial tension of the bath and allowed easier spreading of the particulates as affirmed by Prasanta and Suman [28]. Moreover, Popoola et al. [5] noted that stable adhesion has a better flow than the visible irregular degradation of the latter. Prasanta and Suman [28] and Finazzi et al. [30, 31] also affirmed that metallic particles or composites such as Al_2O_3 reinforcement in the coating also reduced the scaling and increased the wear

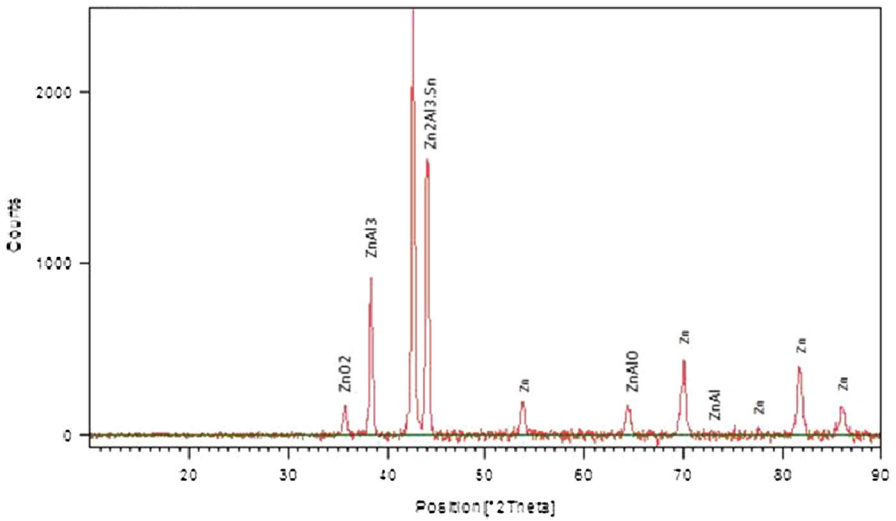

Fig. 5 XRD pattern of Zn with dispatched Al–ST

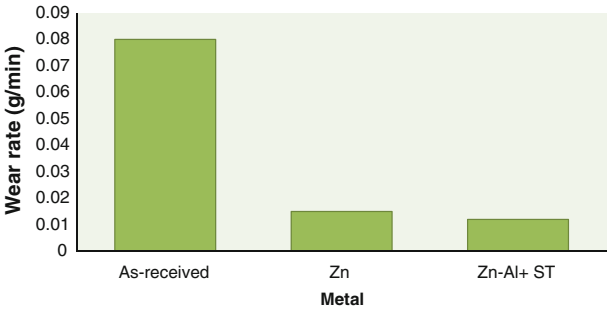

Fig. 6 Variation of wear rate of the uncoated and coated samples

resistance of coatings as compared to the non-reinforced coatings which is in line with the result found in this study.

Hardness analysis

The hardness analysis shown in Fig. 9 was carried out in order to examine the impact of the coating composition on the hardness properties of the Zn-dispatched Al–ST coatings and the ordinary zinc coating. From general observation, the Zn–Al–ST matrix formed a homogeneous composition in the coating layer. The lowest hardness value was obtainable by the Zn deposit which is also a reflection of the damaging effect of the cracked morphology on the hardness properties. According to Popoola et al. [5] and Rahman et al. [23], the micro-hardness of the

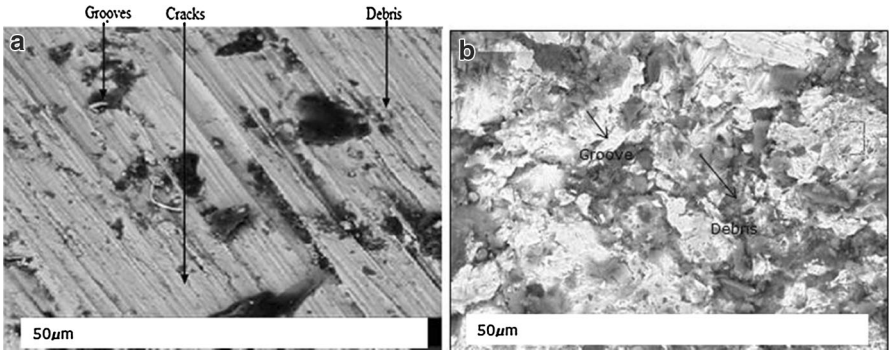

Fig. 7 SEM micrographs of worn surface morphology of **a** as-received sample, **b** Zn coating showing damage region and deep grooves

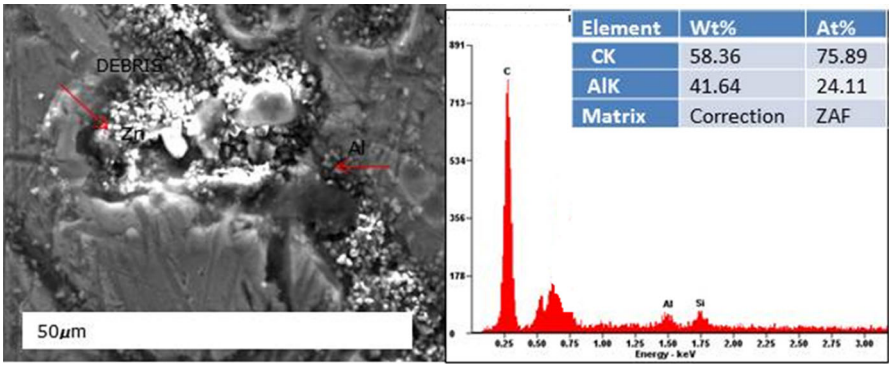

Fig. 8 SEM micrographs of worn surface morphology of Zn deposited in the presence of Al–ST with the EDS

electrodeposited layers can depend on many factors such as electrolyte composition or operating conditions. On this note, the tremendous hardness improvement can be linked to the network of additives that constitute the electrolyte composition for Zn–Al–ST coatings. More interesting is the geometric difference of about 30 % HNV increase above the Zn deposited and the 98 % HNV improvement above the substrate. This justifies the statement by Popoola et al. [4], and Prasanta and Suman [28] that higher hardness value of the coating was due to the fine-grained structure of the deposit or the alloys and the dispersed particles in the fine-grained matrix which may obstruct the easy movement of dislocations, to give a higher hardness value of the deposited samples. Hence, Al and ST are good fine admixed additives for hardness improvement.

AFM analysis results

Scanning AFM was achieved about the surface topography and adhesion phenomena of the Zn–Al–ST and Zn coating samples as shown in Figs. 10 and

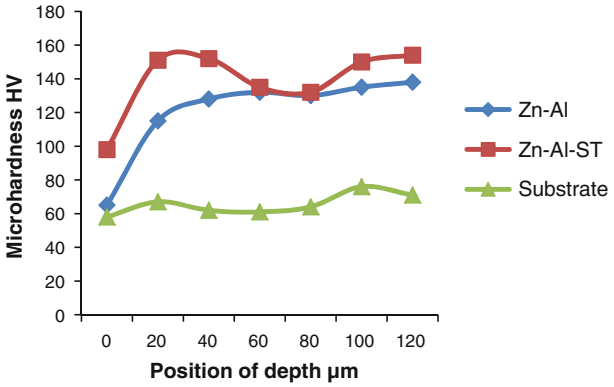

Fig. 9 Variation of microhardness of un-deposited and deposited Zn–Al–ST

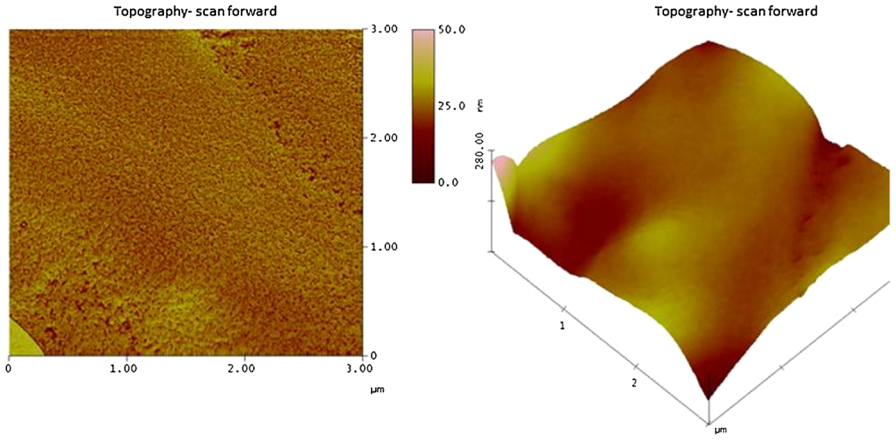

Fig. 10 AFM surface topography of deposited Zn on steel from a chloride bath at 2 A/dm^3 for 20 min at 30 °C without Al–ST

11. It can be observed in Fig. 11 that fine grain size and uniform crystal growth was achieved with crystallites. More significant is the uniform crystal topography and perfect orientation exhibited by the alloy-coated sample, which may be as a result of good metallurgical deposition parameter.

Moreover, Popoola et al. [5] and Finazzi et al. [31] affirmed that surface roughness and adhesion increases most times as a result of the applied voltage on the deposited metal with coalesced crystallite, hence film thicknesses are influenced by metallurgical parameters. For zinc samples in Fig. 10, there is some undulation on the surfaces of the coatings.

Furthermore, it can be seen from the 2D AFM view of Fig. 11 that the lumps projections within the surface interface have shown a more homogeneous diffusion with good coarse grain compatibility compared to the other.

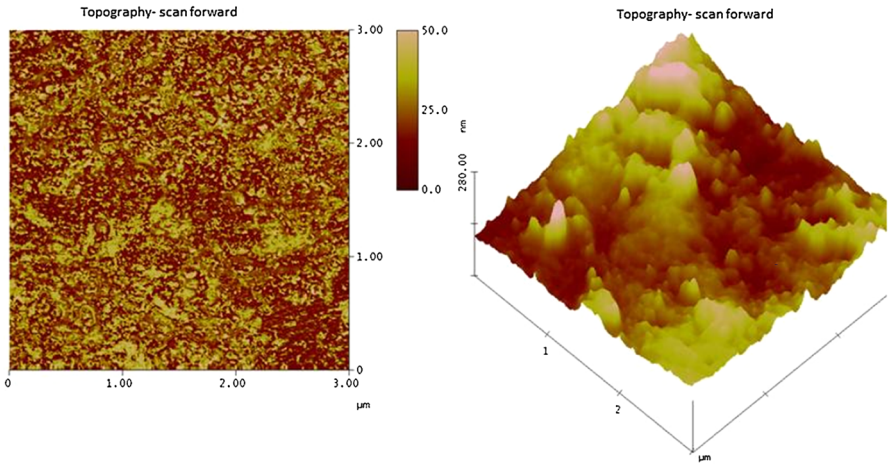

Fig. 11 AFM surface topography of electrodeposited Zn–Al–ST coatings samples from a chloride bath at 2 A/dm^3 for 20 min at 30 °C

Conclusion

- Particulates of Al and ST were uniformly distributed throughout the metal matrix of Zn which contributed to an excellent level of resistance to wear and increase in the hardness value.
- SEM photomicrographs of Zn showed little porosity and stress along the interface. However, there was no evidence of porosity on Zn–Al–ST.
- X-ray diffractograph outcome of the deposits indicates a preferred orientation phase structure of Zn, ZnAlO, and $Zn_2Al_3{\cdot}Sn$.
- The EDS analysis also affirmed the existence of Zn, Al, and other phyto-chemical agents from ST responsible for the adhesion of the deposits on the steel.
- The integration of the particles and the juice extract help in blocking barriers within the cathode by filling the crevices and gaps of the plating.
- SEM macrographs of the deposits in the presence of admixed additives showed no evidence of porosity, and low levels of variation in the deposition interface were seen.

Acknowledgments This material is based upon work supported financially by the National Research Foundation South Africa. Tshwane University of Technology is thanked for equipment and material support.

References

1. O.S.I. Fayomi, A.P.I. Popoola, Int. J Electrochem. Sci **7**, 6570 (2012)
2. O.S. Fayomi, V.R. Tau, A.P.I. Popoola, B.M. Durodola, O.O. Ajayi, C.A. Loto, O.A. Inegbenebor, J. Mater. Environ. Sci. **3**, 280 (2011)
3. H.A. Chitharanjan, K. Venkatakrishna, N. Eliaz, Surf. Coat. Technol. **205**, 2041 (2010)

4. A.P.I. Popoola, O.S.I. Fayomi, O.M. Popoola, Int. J. Electrochem. Sci **7**, 4917 (2012)
5. A.P.I. Popoola, O.S.I. Fayomi, O.M. Popoola, Int. J. Electrochem. Sci **7**, 4860–4870 (2012)
6. M.O.H. Amuda, W. Subair, O.W. Obitayo, Int. J. Eng. Res. Afr. **2**, 39 (2009)
7. M.G. Hosseini, H. Ashassi-Sorkhabi, H. Ghiasvand, Surf. Coat. Technol. **202**, 2904 (2008)
8. C. Mohankumar, K. Praveen, V. Venkatesha, K. Vathsala, O. Nayana, J. Coat. Technol. Res. **9**, 77 (2012)
9. S. Shivakumara, U. Manohar, Y. Arthoba Naik, T.U. Venkatesha, Bull. Mater. Sci. **30**:462 (2007)
10. A.E. Elsherief, M.A. Shoeib, Corros. Prev. Control **50**, 25–30 (2003)
11. B.M. Praveen, T.V. Venkatesha, Int. J. Electrochem. **261**, 410 (2011)
12. T. Dikici, O. Culha, M. Toparli, J. Coat. Technol. Res. **7**, 792 (2010)
13. Q.X. Liu, S. Zein El Abedin, F. Endres, Surf. Coat. Technol. **201**, 1356 (2006)
14. S. Basavanna, Y. Arthoba Naik, J. Appl.Electrochem. **517**(11), 3287–3291 (2012)
15. M.M. Abou-Krisha, F.H. Assaf, S.A. El-Naby, J. Coat. Technol. Res. **6**, 391 (2009)
16. L.M. Regis, N.S.C. Paulo, N.C. Adriana, L.N. Pedro, J. Brazilian Chem. Soc. **23**, 328 (2012)
17. B.C. Tripathy, P. Singh, D.M. Muir, S.C. Das, J. Appl. Electrochem. **31**, 301 (2001)
18. M. Mounga, L. Ricq, G. Douglade, P. Bercot, Surf. Coat. Technol. **201**, 767 (2006)
19. C.A. Loto, I. Olefjord, Corros. Prev. Control J. **39**, 149 (1992)
20. C.A. Loto, Discov. Innov. **5**, 253 (1993)
21. C.A. Loto, I. Olefjord, H. Mattson, Corros. Prev. Control J. **39**, 885 (1991)
22. C.A. Loto, E.T. Odumbo, J Corros. Prev. Control **45**, 553–557 (1989)
23. M.J. Rahman, S.R. Sen, M. Moniruzzaman, K.M. Shorowordi, J. Mech.Eng. **40**, 9–12 (2009)
24. C.N. Panagopoulos, E.P. Georgiou, M.G. Tsoutsouva, M. Krompa, J. Coat. Technol. Res. **8**, 133 (2011)
25. J. Gala, E. Eagiewka, J. Barai-Iska, J. Appl. Electrochem. **11**, 741 (1981)
26. T.V. Byk, T.V. Gaevsaya, Tsybulskaya Surf. Coat. Technol. **202**, 5823 (2008)
27. B. Bobić, S. Mitrović, M.I. Babić, I. Bobić, Tribol Ind. **32**, 11 (2010)
28. S. Prasanta, K.D. Suman, Mater. Des. **32**, 1760 (2011)
29. Q. Zhou, Z. Shao, C. He, Z. Shao, Q. Cai, W. Gao, J. Chin. Soc. Corros. Prot. **27**(1), 27–30 (2007)
30. M. Novaík, D. Vojtech, T. Vitu, Appl. Surf. Sci. **256**(9), 2956–2960 (2010)
31. G.A. Finazzi, E.M. de Oliveira, I.A. Carlos, Sur. Coat. Technol. **187**, 377 (2004)
32. S. Basavanna, Y. Arthoba Naik, J. Appl. Electrochem. **39**(2009), 1975 (1982)